Umklapp scattering is not necessarily resistive

Zhiwei Ding,[1,3] Jiawei Zhou,[1] Bai Song,[1] Mingda Li,[2] Te-Huan Liu,[1] and Gang Chen[1,*]

[1]*Department of Mechanical Engineering, Massachusetts Institute of Technology, Cambridge, Massachusetts 02139, USA*
[2]*Department of Nuclear Science and Engineering, Massachusetts Institute of Technology, Cambridge, Massachusetts 02139, USA*
[3]*Department of Materials Science and Engineering, Massachusetts Institute of Technology, Cambridge, Massachusetts 02139, USA*

Since Peierls's pioneering work, it is generally accepted that phonon-phonon scattering processes consist of momentum-conserving normal scatterings and momentum-destroying Umklapp scatterings, and that the latter always induce thermal resistance. We show in this work that Umklapp scatterings are not necessarily resistive—no thermal resistance is induced if the projected momentum is conserved in the direction of heat flow. This distinction is especially important in anisotropic materials such as graphite and black phosphorous. By introducing a direction-dependent definition of normal and Umklapp scattering, we can model thermal transport in anisotropic materials using the Callaway model accurately. This accuracy is physically rooted in the improved description of mode-specific phonon dynamics. With the new definition, we predict that second sound might persist over much longer distances than previously expected.

I. INTRODUCTION

Phonons are major heat carriers in semiconductors and dielectrics. In crystalline solids, Peierls [1,2] attributed the origin of thermal resistance to the combination of anharmonicity and the discrete nature of crystal lattice. Anharmonicity results in interactions between the lattice vibrational waves, referred to as phonon-phonon scattering processes. However, anharmonicity alone cannot induce resistance, as discussed by Peierls [2]—an infinite thermal conductivity is expected if all the phonon scattering processes conserve momentum. To explain the finite thermal conductivity, Peierls proposed that from the perspective of momentum, phonon-phonon scattering could be divided into two categories: normal scattering (N scattering) [3] and Umklapp scattering (U scattering). An N scattering process conserves the phonon momentum and induces no thermal resistance by itself, and it merely redistributes momentum among different phonon modes. In comparison, U scattering is a momentum-destroying process that leads to thermal resistance [2,4–8]. More specifically, for a three-phonon absorption scattering process, the wave vectors of the three phonons satisfy the following constraint:

$$\mathbf{q} + \mathbf{q}' = \mathbf{q}'' + \mathbf{G}, \qquad (1)$$

where $\mathbf{q}$ and $\mathbf{q}'$ are the wave vectors of the interacting phonons, $\mathbf{q}''$ is the wave vector of the newly created phonon, and $\mathbf{G}$ represents a reciprocal lattice vector or zero vector. The conventional definitions of N scattering and U scattering are illustrated in Fig. 1, where the first Brillouin zone (BZ) is depicted as a square for simplicity. If the wave vector of the new phonon $\mathbf{q}''$ is within the first BZ, the three-phonon interaction conserves momentum and is considered N scattering [Fig. 1(a)]. However, if $\mathbf{q}''$ is outside the first BZ [Fig. 1(b)],

the phonon momentum is not conserved ($\mathbf{G} \neq \mathbf{0}$) and the process is categorized as U scattering [5]. Proper treatment of N scattering and U scattering holds the key to model phonon transport, especially to capture the collective drift motion of phonons [9,10], which characterizes phonon hydrodynamic transport [9,10]—in analogy to the hydrodynamic flow of molecules [11]. Many exotic phenomena of fundamental importance emerge in the hydrodynamic transport regime, such as phonon Poiseuille flow [12,13], Knudsen minimum [5,12], and second sound [14–18].

Major advances in first-principles computations over the last decade have enabled solving the phonon Boltzmann transport equation (BTE) numerically without the distinction between N-scattering and U-scattering processes [19–21]. However, the high computational cost limits the applicability of such exact solution processes to simple materials, where the number of atoms in a unit cell is within computational resource limits. A more affordable approach appropriate for mesoscale structures is to model phonon-phonon interactions using the relaxation time approximation (RTA), which treats all phonon scattering processes as U scattering and represents them with a single lifetime [21–23]. However, the RTA significantly underestimates the thermal conductivity when strong N scattering is present [24]. To correct for this discrepancy, Callaway proposed a new model to separate the effects of N scattering and U scattering on heat transport [8], which can be written as

$$\mathbf{v}_g \cdot \nabla f = -\frac{f - f_0}{\tau_U} - \frac{f - f_d}{\tau_N}, \qquad (2)$$

where f and $\mathbf{v}_g$ denote the phonon distribution function and group velocity, and $\tau_U{}^{-1}$ and $\tau_N{}^{-1}$ represent the U-scattering and N-scattering rates, respectively. While the U-scattering processes relax the phonon distribution to the equilibrium Bose-Einstein distribution f_0, the N-scattering processes facilitate the establishment of a displaced distribution f_d,
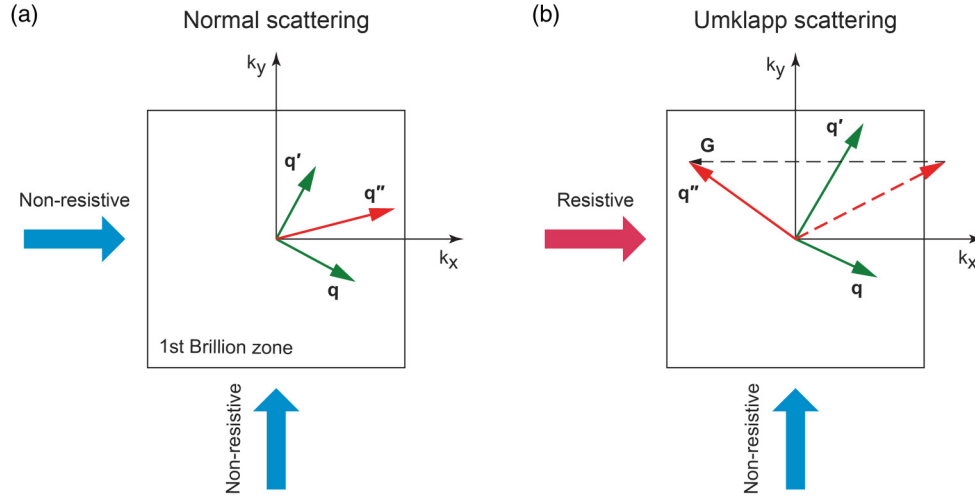
*gchen2@mit.edu

FIG. 1. Schematic illustration of normal scattering (**N**-scattering) and Umklapp scattering (**U**-scattering) processes, as conventionally defined. (a) **N** scattering does not induce thermal resistance in either the x or y direction, while (b) **U** scattering induces resistance in the x direction but not in the y direction.

which can be written as

$$f_d = \frac{1}{\exp\left[\frac{\hbar(\omega - \mathbf{q}\cdot\mathbf{u})}{k_B T}\right] - 1}. \tag{3}$$

Here, $\hbar$, ω, $\mathbf{q}$, k_B, and T denote the reduced Planck's constant, phonon frequency, phonon wave vector, the Boltzmann constant, and temperature, respectively. The collective phonon drift velocity $\mathbf{u}$ is discussed in Ref. [25] and can be determined from the conservation of momentum in N-scattering processes [9]:

$$\sum \frac{f - f_d}{\tau_N} \hbar \mathbf{q} = 0, \tag{4}$$

where the summation is over all phonon modes (same below unless specified). The displaced distribution function is analogous to the BGK approximation for rarefied gas flow [26].

The Callaway model preserves the efficiency of the RTA while significantly approaching the accuracy of the exact solution schemes and has been truly instrumental to phonon transport studies since it was proposed in 1959. Its effectiveness was first demonstrated for modeling thermal conductivities at low temperatures [8,27], especially for phonon hydrodynamics [28,29], such as phonon Poiseuille flow [12], Knudsen minimum [12,30], and second sound [29]. In past studies, all U-scattering processes are grouped into τ_U, i.e., assumed to create resistance to heat flow.

However, not all U scatterings as conventionally defined (Fig. 1) create thermal resistance. In fact, a U-scattering process does not really cause any thermal resistance if the projection of the phonon momentum involved in the scattering is conserved in the heat flow direction. For example, the U-scattering event shown in Fig. 1(b) only induces resistance to heat flow in the x direction, but not in the y direction. We will show later that this distinction is especially important for anisotropic materials. We hereby propose that a proper classification of N scattering and U scattering should be based on the projected phonon momentum in the heat flow direction. A scattering process should be considered N scattering as long as the phonon momentum is conserved in the direction of heat

flow. With this understanding, Eq. (1) should be rewritten as

$$\mathbf{q}_j + \mathbf{q}'_j = \mathbf{q}_j'' + \mathbf{G}_j, \tag{5}$$

where j represents the heat transport direction, $\mathbf{q}_j$ and $\mathbf{G}_j$ represent the projections of vectors $\mathbf{q}$ and $\mathbf{G}$ along j. A scattering event is N scattering as long as $\mathbf{G}_j = 0$, which holds when $\mathbf{G} = \mathbf{0}$ or $\mathbf{G}$ is a reciprocal lattice vector orthorgonal to j. Therefore, all the conventional N-scattering processes remain N scattering with the new definition, but some scattering processes originally catergorized as U scatteirng are now classified as N scattering. To avoid confusion, we denote the heat transport direction-dependent N- and U-scattering processes as N_j and U_j scattering. In what follows, by comparing with the exact solutions of the phonon BTE, we demonstrate that the proposed new classification of N-scattering and U-scattering processes leads to much more accurate predictions of thermal conductivity using the Callaway model. We then conclude with a discussion of the significant consequence of the new definition on the propagation length of second sound in the phonon hydrodynamic transport regime.

II. RESULTS AND DISCUSSIONS

A. Thermal conductivity

We use black phosphorus (BP) and graphite as the prototypical materials to demonstrate how our new definition can improve the performance of the Callaway model. These two materials are chosen because they are representative of anisotropic two-dimensional (2D) and 3D materials with one primitive vector orthogonal to the others. The atomic structures of the two materials are shown as insets of Fig. 2. The computed thermal conductivity of BP along the zigzag (ZZ) direction and graphite in the basal plane direction are plotted in Fig. 2 as a function of temperature. We focus on transport in these directions because the transport property in the armchair (AM) direction of BP and the cross-plane direction of graphite is insensitive to the treatment of N and U scattering (Fig. S1). Here we compare the thermal conductivities predicted using
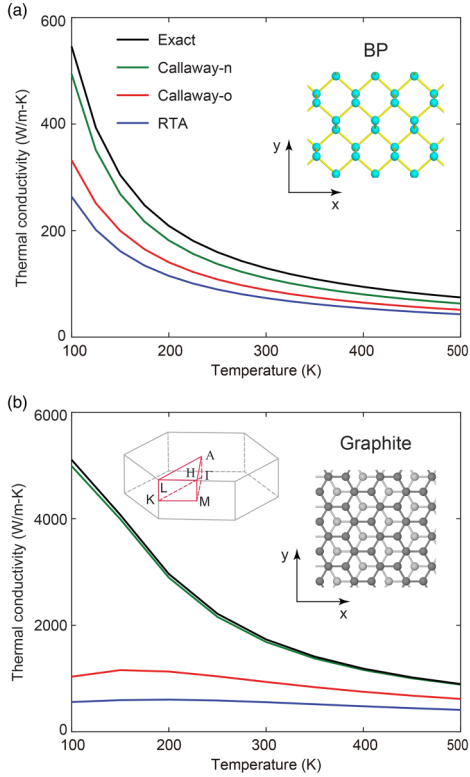
FIG. 2. Thermal conductivity of (a) BP in the zigzag direction and (b) graphite in the basal direction. Insets show atomic structures of BP and graphite, as well as the reciprocal space for graphtie.

four different methods: (1) iterative numerical soluton to the BTE which is exact and serves as the reference, (2) Callaway model with the new definition of N and U scattering, i.e., N_j and U_j scattering, (3) Callaway model with the original definition of N and U scattering, and (4) RTA. All the scattering rates were obtained from first-principles calculations. The details for computing thermal conductivity using RTA, Callaway, and the iterative method can be found in Ref. [31]. One can see that both the RTA and the Callaway model with the original definition of N- and U-scattering rates underestimate the thermal conductivity across the wide temperature range considered (100 K−500 K). With the new definition, the performance of the Callaway model improves significantly at all temperatures. For graphite in particular, the calculated thermal conductivity using the Callaway model with the new definition is less than 3% smaller than the exact value. In addition, the kinetic collective model (KCM) proposed by Guyer and Krumhansl [9,32] has been successfully used to predict the thermal conductivity of several materials [33,34]. Similar to the Callaway model, the accuracy of KCM also depends on the accuracy of N- and U-scattering rates and improves with the new definition (Fig. S2). This further demonstrates the validity of our new definition.

B. Effective phonon lifetime

For a more detailed picture, we define an effective phonon lifetime as

$$\tau = \frac{f - f_0}{\frac{\partial T}{\partial x} \frac{\partial f_0}{\partial T} v_x}, \tag{6}$$

where f is the phonon mode distribution obtained by solving BTE with a temperature gradient $\partial T/\partial x$ in the x direction. With this effective lifetime, one can readily obtain thermal conductivity via the phonon gas model. In Fig. 3, we can see that the RTA and the Callaway model with the original definition of N and U scattering not only underestimate the effective phonon lifetime, but also lead to effective lifetime distributions that are dramatically different from the exact solution. In contrast, the performance of the Callaway model substantially improves when combined with the N_j- and U_j-scattering rates. In particular, we highlight the region enclosed by the white semicircle. Phonons in this region are most strongly affected by our modification of the definition of N and U scattering. Based on the conventional definition of U scattering, phonons with wave vectors near the zone boundary are prone to U scattering with ($\mathbf{G} \neq 0$) in Eq. (1). However, our new definition treats a phonon scattering event as N_j scattering as long as the projection of $\mathbf{G}$ in the heat transport direction j is zero. For example, in BP a phonon with large q_y is prone to U scattering with $\mathbf{G} = \mathbf{G_y}$ in Eq. (1), where $\mathbf{G_y}$ is the lattice vector in the reciprocal space along the k_y direction. However, this process should be considered as N_j scattering if heat transport along the x direction is of interest, as the momentum in the x direction is conserved [$\mathbf{G_j} = 0$ in Eq. (5)]. Such difference is clearly observed in the distribution of U-scattering percentage in the reciprocal space shown in Fig. 4. For phonons with small q_y, the percentage of U-scattering rates remains almost unchanged with the modification of definition, while the percentage of U-scattering rates significantly reduces for phonons with large q_y (Fig. 4). A similar analysis was also performed in graphite for phonons with large q_z [Figs. 3(e)–3(h) and Fig. S3].

C. Second sound propagation length

Beyond diffusive transport, phonon hydrodynamic transport has been of great fundamental interest for decades and has recently drawn much revived attention [12,28,35–37]. The Callaway model has been widely employed to investigate many of the characteristic phenomena in hydrodynamic transport such as phonon Poiseuille flow [12,35], second sound [28,29,37], phonon Knudsen minimum [12,30] and phonon viscous flow [38]. Second sound refers to the propogation of heat in a phonon gas, in analogy to the propogation of ordinary sound waves in solids [39,40]. Second sound is of particular interest [40] in thermal transport since it is the most direct demonstration that heat can travel as waves, in contrast to the diffusion process underlying the Fourier heat conduction law. This phenomenon results from the collective phonon motion established by N scattering when it dominates over U scattering. Second sound has been experimentally observed at cryogenic temperatures by first applying a heat pulse on one end of a sample then measuring the transient temperature response on the opposite end [16,18,41,42]. The velocity and propagation length of second sound are two critical characteristics for experimental observations. Following Refs. [43,44], and using the energy and momentum conservation equations derived from BTE, the second sound velocity $\boldsymbol{v}$ and propagation length l in the x direction can be written
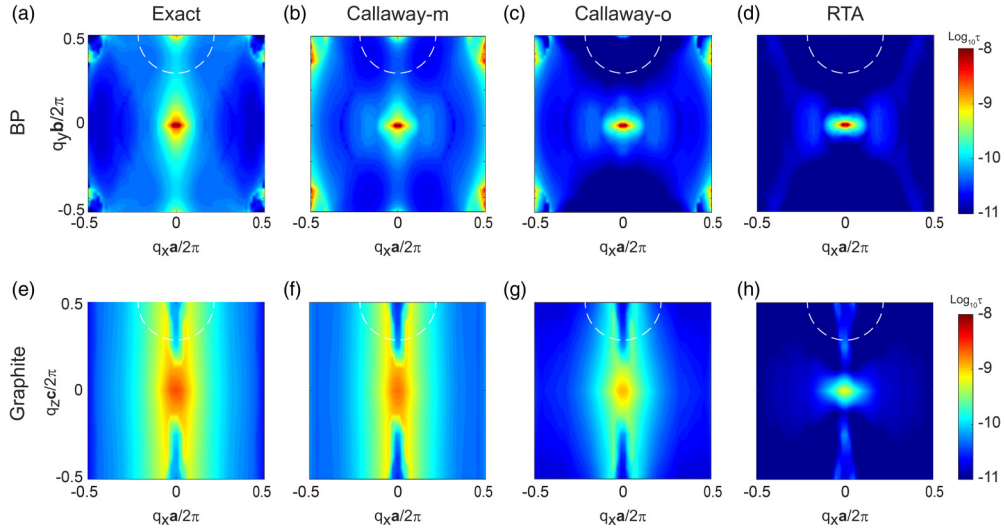
FIG. 3. Effective lifetime at 300 K under a tempeature gradient in the x direction obtained for BP (a)–(d) and graphite (e)–(h) based on (a)–(e) exact iterative solution; (b), (f) the Callaway model with new definition of N- and R-scattering rates; (c), (g) the Callaway model with orignal definition; and (d), (h) the RTA model. For phonons enclosed by the white semicircle at the zone boundary in the y direction, conventional U-scattering events can readily take place. However, these scatterings are considered N-scatterings based on the new definition.

as [45]

$$v^2 = \frac{\left(\sum \frac{C_q q_x v_x}{\omega}\right)^2}{\sum \frac{C_q q_x^2}{\omega^2} \sum C_q}, \tag{7}$$

$$l = \frac{2v \sum \frac{C_q q_x^2}{\omega^2}}{\sum \frac{C_q q_x^2}{\omega^2 \tau_U}}, \tag{8}$$

where C_q is the mode heat capacity. The propagation lengths of second sound in BP and graphite predicted using both the original and the new definition are shown in Fig. 5. One can see that using our new definition, the predicted propagation lengths in both BP and graphite are almost an order of magnitude larger, which indicates the necessity of our new definition in studying phonon hydrodynamic transport.

D. The role of anisotropy

The new interpretation regarding whether a phonon-scattering process should be viewed as a U-scattering process is particularly critical in anisotropic materials, where phonons dispersion along one direction (denoted as "soft" axis) is much softer than the other directions ("stiff" directions). For example, in graphite, the weak interlayer van der Waals (vdW) interactions lead to nearly flat dispersion along the cross-plane direction. In such a case, if one considers heat flow along the stiff axis (e.g., in-plane direction for graphite), there will be significant phonon scatterings involving phonons along the "soft" axis, due to the large scattering phase space provided by the flat phonon band along this axis [46] and their high phonon occupations resulting from the low phonon frequencies. Therefore, phonons as shown in Fig. S4(b) suffer from a large amount of scatterings with $\mathbf{G} = \mathbf{G_{cross}}$ [see Eq. (1), where $\mathbf{G_{cross}}$ is the lattice vector in the reciprocal
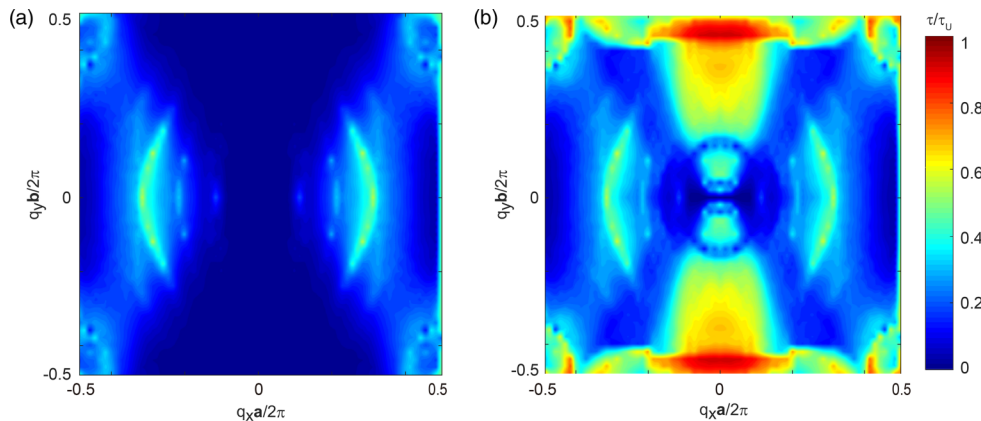

FIG. 4. Distribution of U-scattering percentage in the reciprocal space for BP with (a) new definition and (b) original definition of N- and U-scattering at 300 K, under a temperature gradient in the x direction.
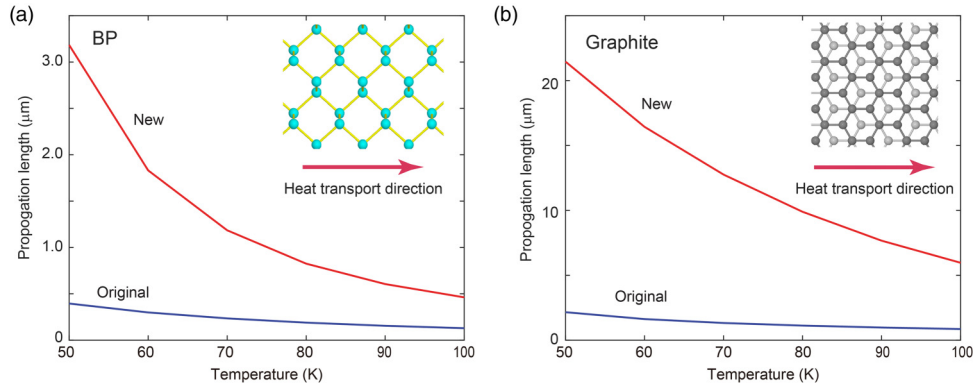
FIG. 5. Propagation length of second sound as a function of temperature computed using the Callaway model with different definitions of N-scattering and U-scattering in (a) BP and (b) graphite.

space along the cross-plane direction], which are regarded as a U-scattering process based on the conventional wisdom, but have no effect on heat flow along the stiff direction in our revised picture.

III. CONCLUSION

In summary, we have shown that, contrary to conventional wisdom pioneered by Peierls, not all U-scattering processes are resistive. Whether or not a U-scattering event contributes to thermal resistance depends on its projection to the heat flow direction. A U-scattering process causes thermal resistance only when the projected momentum is not conserved. This distinction is crucial in anisotropic materials. Using the new definition of N scattering and U scattering, we show that the Callaway model combined with the first-principles calculations gives a much more precise prediction of the total thermal conductivity and the mode-specific properties as well. By showing its substantial effects on second sound propagation length, we also highlight the potential impact of our new definition on the study of phonon hydrodynamic transport.

IV. METHODS

A. Computational Details.

The computational details for BP and graphite follow those in Refs. [47] and [12], respectively. Briefly, for BP, calculations were carried out using the Quantum ESPRESSO package [48]. The ultrasoft pseudopotential with Perdew–Burke–Ernzerhof (PBE) exchange–correlation functional was employed to describe the interactions between the phosphorus atoms. For graphite, computations were performed by using the Vienna *Ab initio* Simulation Package [49–51] with projector-augmented-wave pseudopotentials and local density approximation for the exchange-correlation energy functional. To include the vdW interactions between layers in graphite, we used an explicit nonlocal functional of density named optB88 functional [52,53]. In addition, the third-order force constants of BP were calculated using a real-space supercell approach with a 5×4×1 supercell and a 2×2×1 k-grid, considering the fifth-nearest neighbors.

B. N-scattering and U-scattering rates

The phonon-phonon scattering rate due to anharmonicity is given by [54]

$$
\Gamma^{\pm}_{\lambda\lambda'\lambda''} = \frac{\hbar\pi}{4N_p} \frac{f'_0 \mp f''_0 + 1/2 \mp 1/2}{\omega_\lambda \omega_{\lambda'} \omega_{\lambda''}}
$$

$$
\times |V^{\pm}_{\lambda\lambda'\lambda''}|^2 \delta(\omega_\lambda \pm \omega_{\lambda'} - \omega_{\lambda''}), \qquad (9)
$$

where λ represents $(n, \mathbf{q})$ with n being the branch number and $\mathbf{q}$ the phonon wave vector, "+" and "−" correspond, respectively, to phonon absorption and emission, f'_0 stands for $f_0(\omega_{\lambda'})$, and N_p is the total number of grid points. Energy conservation is enforced by the Dirac delta function. The three-phonon scattering matrix $V^{\pm}_{\lambda\lambda'\lambda''} = V(n, \mathbf{q}; n', \pm\mathbf{q}'; n'', \mathbf{q}'')$ is given by [54]

$$
V(n, \mathbf{q}; n', \mathbf{q}'; n'', \mathbf{q}'') = \sum_k \sum_{l'k'} \sum_{l''k''} \sum_{\alpha\beta\gamma} \Phi^{0,k;l',k';l'',k''}_{\alpha\beta\gamma} e^{i\mathbf{q}'\cdot\mathbf{R}_{l'}}
$$

$$
\times e^{i\mathbf{q}''\cdot\mathbf{R}_{l''}} \frac{\xi^n_{\alpha k}(\mathbf{q})\xi^{n'}_{\beta k'}(\mathbf{q}')\xi^{n''}_{\gamma k''}(\mathbf{q}'')}{\sqrt{m_k m_{k'} m_{k''}}}, \qquad (10)
$$

where $\mathbf{R}'_l$ is the lattice vector, and m_k is the mass of the kth atom, $\Phi^{0,k;l',k';l'',k''}_{\alpha\beta\gamma}$ is the third-order force constant, and $\xi^n_{\alpha k}(\mathbf{q})$ is the α component of the eigenvector of phonon branch n with wave vector $\mathbf{q}$.

The phonon-phonon scattering rate can be calculated as

$$
\tau^{-1}_{\lambda,\, N/U} = \sum_{\lambda'\lambda'' \in S_{N/U}} \left(\Gamma^+_{\lambda\lambda'\lambda''} + \frac{1}{2}\Gamma^-_{\lambda\lambda'\lambda''} \right), \qquad (11)
$$

The summation is over all phonon mode indices λ', λ'', satisfying

$$
\mathbf{q}_\lambda \pm \mathbf{q}_{\lambda'} = \mathbf{q}_{\lambda''} + \mathbf{G} \qquad (12)
$$

where "+" and "−" correspond to constraints for $\Gamma^+_{\lambda\lambda'\lambda''}$ and $\Gamma^-_{\lambda\lambda'\lambda''}$, accordingly, and $\mathbf{G}$ represents a reciprocal lattice vector. If $\mathbf{G} = 0$, the summation gives N-scattering rates, while

U-scattering rates are obtained if we set $\mathbf{G} \neq \mathbf{0}$. In our new definition, $\mathbf{G_j}$, the projection of $\mathbf{G}$ along the heat transport direction is used instead. If $\mathbf{G_j} = 0$, the summation gives N-scattering rates, while U-scattering rates are obtained if we choose $\mathbf{G_j} \neq 0$.

[1] V. R. Peierls, Ann. Phys. **395**, 1055 (1929).

[2] R. E. Peierls, *Quantum Theory of Solids* (Oxford University Press, Oxford, 1955).

[3] Normal scattering process was named later by Callaway in Ref. [8].

[4] A. A. Maznev and O. B. Wright, Am. J. Phys. **82**, 1062 (2014).

[5] G. Chen, *Nanoscale Energy Transport and Conversion: A Parallel Treatment of Electrons, Molecules, Phonons, and Photons* (Oxford University Press, Oxford, 2005).

[6] L. Lou, *Introduction to Phonons and Electrons* (World Scientific, Singapore, 2003).

[7] Z. M. Zhang, *Nano/Microscale Heat Transfer* (McGraw Hill, New York, 2007).

[8] J. Callaway, Phys. Rev. **113**, 1046 (1959).

[9] R. A. Guyer and J. A. Krumhansl, Phys. Rev. **148**, 778 (1966).

[10] J. C. Ward and J. Wilks, London, Edinburgh, Dublin Philos. Mag. J. Sci. **43**, 48 (1952).

[11] M. Knudsen, Ann. Phys. **333**, 75 (1909).

[12] Z. Ding, J. Zhou, B. Song, V. Chiloyan, M. Li, T. H. Liu, and G. Chen, Nano Lett. **18**, 638 (2018).

[13] L. P. Mezhov-Deglin, Sov. Phys. JETP **22**, 47 (1966).

[14] J. Ranninger, J. Phys. C: Solid State Phys. **2**, 929 (1969).

[15] H. E. Jackson, C. T. Walker, and T. F. McNelly, Phys. Rev. Lett. **25**, 26 (1970).

[16] A. Koreeda, R. Takano, and S. Saikan, Phys. Rev. Lett. **99**, 265502 (2007).

[17] V. Narayanamurti and R. C. Dynes, Phys. Rev. Lett. **28**, 1461 (1972).

[18] D. W. Pohl and V. Irniger, Phys. Rev. Lett. **36**, 480 (1976).

[19] G. Fugallo, M. Lazzeri, L. Paulatto, and F. Mauri, Phys. Rev. B **88**, 045430 (2013).

[20] D. A. Broido, M. Malorny, G. Birner, N. Mingo, and D. A. Stewart, Appl. Phys. Lett. **91**, 231922 (2007).

[21] K. Esfarjani, G. Chen, and H. T. Stokes, Phys. Rev. B **84**, 085204 (2011).

[22] L. Lindsay, D. A. Broido, and T. L. Reinecke, Phys. Rev. B **87**, 165201 (2013).

[23] J. Carrete, B. Vermeersch, A. Katre, A. van Roekeghem, T. Wang, G. K. H. Madsen, and N. Mingo, Comput. Phys. Commun. **220**, 351 (2017).

[24] A. Ward, D. A. Broido, D. A. Stewart, and G. Deinzer, Phys. Rev. B **80**, 125203 (2009).

[25] P. G. Klemens, Handb. der Phys. **14**, 198 (1956).

[26] P. L. Bhatnagar, E. P. Gross, and M. Krook, Phys. Rev. **94**, 511 (1954).

[27] J. A. Krumhansl, Proc. Phys. Soc. **85**, 921 (1965).

[28] A. Cepellotti, G. Fugallo, L. Paulatto, M. Lazzeri, F. Mauri, and N. Marzari, Nat. Commun. **6**, 6400 (2015).

[29] S. Lee and L. Lindsay, Phys. Rev. B **95**, 184304 (2017).

[30] Y. Guo and M. Wang, Phys. Rev. B **96**, 134312 (2017).

[31] J. Ma, W. Li, and X. Luo, Phys. Rev. B **90**, 035203 (2014).

[32] R. A. Guyer and J. A. Krumhansl, Phys. Rev. **148**, 766 (1966).

[33] C. De Tomas, A. Cantarero, A. F. Lopeandia, and F. X. Alvarez, J. Appl. Phys. **115**, 164314 (2014).

[34] P. Torres, A. Torelló, J. Bafaluy, J. Camacho, X. Cartoixà, and F. X. Alvarez, Phys. Rev. B **95**, 165407 (2017).

[35] S. Lee, D. Broido, K. Esfarjani, and G. Chen, Nat. Commun. **6**, 6290 (2015).

[36] V. Martelli, J. L. Jiménez, M. Continentino, E. Baggio-Saitovitch, and K. Behnia, Phys. Rev. Lett. **120**, 125901 (2018).

[37] M. Markov, J. Sjakste, G. Barbarino, G. Fugallo, L. Paulatto, M. Lazzeri, F. Mauri, and N. Vast, Phys. Rev. Lett. **120**, 075901 (2018).

[38] M.-Y. Shang and J.-T. Lü, arXiv:1803.08372.

[39] A. Cepellotti and N. Marzari, Phys. Rev. Mater. **1**, 045406 (2016).

[40] D. Joseph and L. Preziosi, Rev. Mod. Phys. **61**, 41 (1989).

[41] C. C. Ackerman, B. Bertman, H. A. Fairbank, and R. A. Guyer, Phys. Rev. Lett. **16**, 789 (1966).

[42] T. F. McNelly, S. J. Rogers, D. J. Channin, R. J. Rollefson, W. M. Goubau, G. E. Schmidt, J. A. Krumhansl, and R. O. Pohl, Phys. Rev. Lett. **24**, 100 (1970).

[43] E. W. Prohofsky and J. A. Kaumrransl, Phys. Rev. **133**, A1403 (1964).

[44] R. J. Hardy, Phys. Rev. B **2**, 1193 (1970).

[45] See Supplemental Material at http://link.aps.org/supplemental/10.1103/PhysRevB.98.180302 for the detailed derivation.

[46] W. Li and N. Mingo, Phys. Rev. B **91**, 144304 (2015) .

[47] T.-H. Liu and C.-C. Chang, Nanoscale **7**, 10648 (2015).

[48] P. Giannozzi, S. Baroni, N. Bonini, M. Calandra, R. Car, C. Cavazzoni, D. Ceresoli, G. L. Chiarotti, M. Cococcioni, I. Dabo, A. Dal Corso, S. de Gironcoli, S. Fabris, G. Fratesi, R. Gebauer, U. Gerstmann, C. Gougoussis, A. Kokalj, M. Lazzeri, L. Martin-Samos, N. Marzari, F. Mauri, R. Mazzarello, S. Paolini, A. Pasquarello, L. Paulatto, C. Sbraccia, S. Scandolo, G. Sclauzero, A. P. Seitsonen, A. Smogunov, P. Umari, and R. M. Wentzcovitch, J. Phys.: Condens. Matter **21**, 395502 (2009).

[49] G. Kresse and J. Furthmüller, Comput. Mater. Sci. **6**, 15 (1996).

[50] G. Kresse, J. Furthmüller, and J. Hafner, Europhys. Lett. **32**, 729 (1995).

[51] G. Kresse and D. Joubert, Phys. Rev. B **59**, 1758 (1999).

[52] J. Klimeš, D. R. Bowler, and A. Michaelides, J. Phys.: Condens. Matter **22**, 022201 (2009).

[53] J. J. Klimeš, D. R. Bowler, and A. Michaelides, Phys. Rev. B **83**, 195131 (2011).

[54] J. M. Ziman, *Electrons and Phonons: The Theory of Transport Phenomena in Solids* (Oxford University Press, Oxford, 1960).